

Hydroformylation of 1,2- and 1,4-Polybutadiene and Their Mixtures with Hydridocarbonyltris(triphenylphosphine)rhodium(I) Catalyst and Excess Triphenylphosphine

Samuel J. Tremont* and Edward E. Remsen

Monsanto Company, Central Research Laboratories, 800 N. Lindbergh Boulevard, St. Louis, Missouri 63167

Patrick L. Mills

Washington University, Department of Chemical Engineering, 1 Brookings Drive, Campus Box 1198, St. Louis, Missouri 63130. Received June 6, 1989; Revised Manuscript Received October 2, 1989

ABSTRACT: The hydroformylation of 1,4-*cis*-polybutadiene, 1,2-syndiotactic polybutadiene, and a mixed polybutadiene containing 12 wt % 1,2-syndiotactic and 88 wt % 1,4-*cis* + *trans* isomers using hydridocarbonyltris(triphenylphosphine)rhodium(I) homogeneous catalyst precursor with excess triphenylphosphine is examined. Through the use of ^{13}C and ^1H NMR spectroscopy, it is shown that hydroformylation of the 1,4-*cis*-polybutadiene using a PPh_3/Rh molar ratio of ca. 165 at 353 K and 2066 kPa of 1:1 CO/H_2 results in the exclusive formation of the internally branched aldehyde product. Hydroformylation of the 1,2-syndiotactic polybutadiene under similar reaction conditions is shown to yield the terminal-branched aldehyde as the major product, with a trace amount of the iso-branched product. The aldehyde products obtained from the mixed polybutadiene system correspond to those obtained for the pure constituents. Comparison of kinetic data derived from gas uptake measurements shows that the initial reaction rate for hydroformylation of 1,2-syndiotactic polybutadiene is about six times greater than that obtained for hydroformylation of 1,4-*cis*-polybutadiene.

Introduction

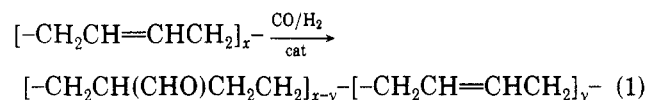
Catalytic methods for synthesizing functionalized polymers that control both the degree of functional group addition and the molecular weight distribution of the resulting polymer are extremely useful for producing a broad range of specialty polymer products. An interesting example is the hydroformylation of polybutadiene, which has been studied by using both homogeneous cobalt^{1,2} and rhodium^{3,4} catalyst precursors.

Our interest in this area evolved from the need to couple nylon block polymers with a suitable rubber phase to yield modified nylon block copolymers having specific physical and chemical properties.⁵⁻⁷ The key reactions are shown in Figure 1. In this case, the polyols represent a modifier that primarily affects the impact strength and the tensile elongation. The nylon blocks control both the crystallinity and heat resistance of the copolymer. Additional details are given by Hedrick and co-workers⁷ who found that low molecular polyols were the preferred rubber phase for their particular reaction injection molding (RIM) application. The polyols used in the early stages of this work were based upon a process in which polybutadiene is functionalized with hydroxyl groups by using free radical chain initiation and termination with hydrogen peroxide.

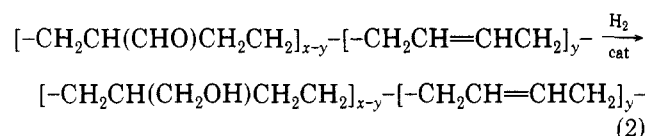
Catalytic hydroformylation of a selected polybutadiene having a known molecular weight distribution and overall composition followed by selective catalytic hydrogenation of the aldehyde functionality provides an alternate approach for producing polyols. This concept is related to the synthesis of oxo alcohols in which olefins are hydroformylated to aldehydes by using homoge-

neous cobalt or rhodium catalysts with subsequent hydrogenation using heterogeneous catalysts.⁸ If 1,4-polybutadiene was selected as the polymer backbone and the appropriate catalyst and reaction conditions were selected, the following polymer functionalization reactions would be expected to occur:

hydroformylation of 1,4-polybutadiene



hydrogenation of the 1,4-hydroformylated product



An analogous set of reactions could be set forth for 1,2-polybutadienes and other related polyolefins. In either case, the above approach provides the basis for obtaining polyol rubber phases with the appropriate characteristics needed for synthesis of modified nylon 6 block copolymers as well as other related specialty polymers.

The primary objective of this study is to examine the hydroformylation of various polybutadienes using hydridocarbonyltris(triphenylphosphine)rhodium(I) catalyst precursor with excess triphenylphosphine ligand. Use of excess ligand is particularly important since its presence should presumably reduce or eliminate olefin isomerization and control the degree of normal to iso aldehyde ratio by analogy to the hydroformylation of monomeric olefins.^{9,10} Although the hydroformylation of polybuta-

* Author to whom correspondence should be addressed.

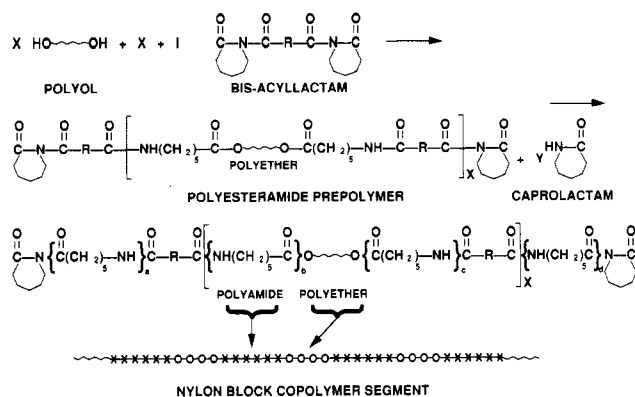


Figure 1. Key chemical reactions in the synthesis of nylon block copolymers from polyols and bis(acylactam) for a reaction injection molding (RIM) application.

dienes with $\text{HRhCO}(\text{PPh}_3)_3$ catalyst has been reported in the literature,^{3,4} no synthesis or kinetic results are available where this same catalyst has been used with high excess triphenylphosphine for the hydroformylation of 1,2-polybutadiene, 1,4-polybutadiene, and commercially available mixed 1,2- and 1,4-polybutadienes. Besides examining the regioselectivity of these systems, the reaction rates for these three polybutadienes were examined in a limited study. Characterization of the polybutadiene precursors and the hydroformylated products using ^{13}C and ^1H NMR as well as gel permeation chromatography will provide insight into the polymer microstructure and how

the particular catalyst system adds the aldehyde functionality to the polymer backbone.

Experimental Section

Apparatus. A diagram of the reaction system that was used to perform the polybutadiene hydroformylation reaction experiments is given in Figure 2. The system components were located within a suitable containment room at the Monsanto High Pressure Experimental Facility with provisions for remote operation of all key valves for operator safety. An Autoclave Engineers 0.3-L autoclave constructed of Hastelloy C was used for all of the reaction experiments. It was operated at constant gas pressure by using a batch liquid. Since the polymer-solvent mixture is non-newtonian and exhibits a greater apparent viscosity than typical organic monomer reactants, the mixing pattern of the gas bubbles in the mixture was visually observed by using a glass vessel whose internal dimensions matched those of the original one. Although the bubbles were less mobile in the polymer-solvent mixture in comparison to the solvent, the differences were not significant enough to justify altering the reactor internals in subsequent reaction experiments.

The reactant gases (carbon monoxide and hydrogen) and inert gases (argon or nitrogen) were piped to the primary gas manifold from high-pressure ($P \geq 27\,579\text{ kPa}$) laboratory cylinders. The large reservoir (LR in Figure 2) was used to store the reactant gas mixture at pressures in excess of 20 684 kPa. During a polybutadiene hydroformylation experiment, the CO/H_2 gas mixture could be intermittently charged to the small reservoir (SR in Figure 2) by a manually operated air valve. The CO/H_2 mixture flowed to the autoclave from the small reservoir through a series of valves and a Tescom dome-loaded regulator that maintained the reactor head space at a constant pressure. The volume of the small reservoir and associated tubing lead-

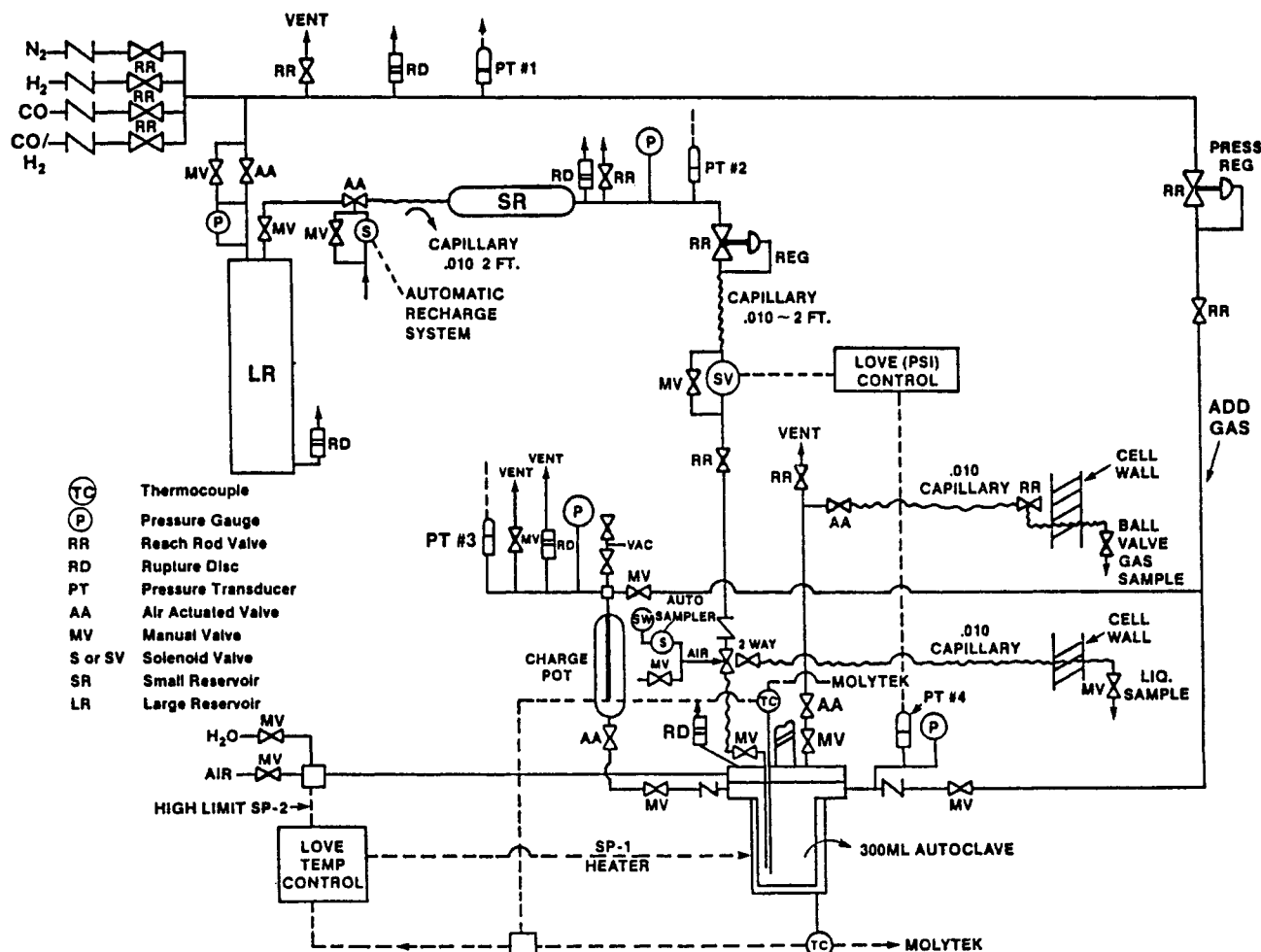


Figure 2. High-pressure batch autoclave system used for the polybutadiene hydroformylation reaction experiments.

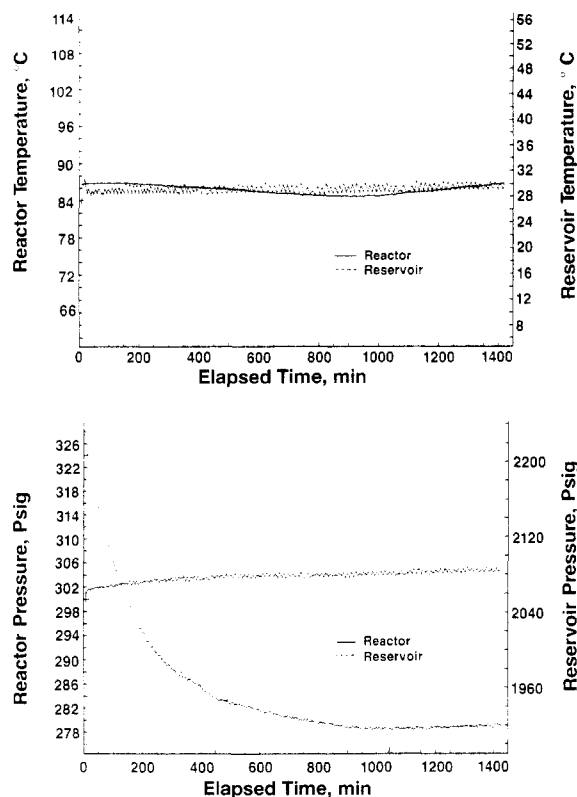


Figure 3. Typical raw experimental reactor performance data obtained during a polybutadiene hydroformylation experiment. (a) Reactor and small reservoir temperatures versus batch reaction time. (b) Reactor and small reservoir pressures versus batch reaction time. Reaction conditions: $C_{PO} = 1.809$ mol/L, $C_{cat} = 3.54 \times 10^{-4}$ mol/L, PPh_3/Rh (M) = 165/1, $P = 2066$ kPa (gauge), $CO/H_2 = 1/1$, $T = 360$ K, solvent = toluene.

ing to the pressure regulator, which was needed for subsequent hydroformylation reaction rate measurements, was precisely determined by the traditional technique of gas pressure equilibration from a known volume.¹¹

The gas pressures in the small reservoir, large reservoir, and autoclave were measured by pressure transducers (Validyne) that had an absolute accuracy of ± 68.9 kPa. The autoclave was heated by the standard single-zone tubular that was supplied with the autoclave. A constant flow of air was directed through the internal coils of the autoclave to remove the excess heat of reaction and to minimize temperature overshoots associated with the significant thermal capacity of the autoclave. The instantaneous temperature of the batch liquid was maintained to within ± 2 K of the desired set point by a PID (Love) temperature controller where the average temperature of the autoclave outer wall and the liquid batch was used as the control input.

Logging of the elapsed batch reaction time, various pressures, and temperatures was performed by a strip chart recorder (Molytek) connected to a microprocessor-based data storage device. Upon completion of an experiment, the stored data were uploaded to a VAX 8600 for data reduction and analysis. The graphical output of the instantaneous temperatures and pressures in the small reservoir and reactor for a typical polymer hydroformylation kinetics experiment is shown in Figure 3. The raw data used to construct the figure were employed in subsequent reaction rate calculations, which are described in Appendix B.

Materials. The mixed polybutadiene used in this work had a microstructure consisting of 10–15 wt % 1,2-polybutadiene, 50–60 wt % *trans*-1,4-polybutadiene, 25–35 wt % *cis*-1,4-polybutadiene, and residual (≤ 0.5 wt %) toluene. It was obtained from Revertex Ltd. and is commercially produced by the anionic polymerization of butadiene monomer using organolithium catalysts in toluene reaction solvent and is denoted by LX-16. The *cis*-1,4-polybutadiene was obtained from Aldrich and had a purity in excess of 99 wt %. The 1,2-polybutadiene was purchased from Polysciences and contained 90% syndiotactic isomer with

Table I
Molecular Weight Averages of the Polybutadiene Reactants^a

reactant	$10^{-3}\bar{M}_n$	$10^{-3}\bar{M}_w$	$P = \bar{M}_w/\bar{M}_n$
LX-16	5.2	7.2	1.38
1,4- <i>cis</i> -polybutadiene	67.91	156.8	2.30
1,2-syndiotactic polybutadiene	21.80	45.79	2.10

^a Determined by gel permeation chromatography.

ca. 10 wt % *cis* + *trans*-1,4-polybutadiene. The molecular weight averages of each were determined by gel permeation chromatography (described below) and are summarized in Table I. The measured values of the number-average molecular weights are in reasonable agreement with those cited by their sources.

The hydroformylation catalyst precursor, hydridocarbonyltris(triphenylphosphine)rhodium(I), $HRhCO(PPh_3)_3$, was obtained from Strem Chemicals. Although the purity was not explicitly given, it was a crystalline grade material with a probable purity in excess of 99 mol %. Triphenylphosphine ligand, which was added to the reaction mixture to achieve a predetermined PPh_3/Rh molar ratio for selectivity control, was obtained from Aldrich. It was recrystallized from ethanol to reduce the presence of polar organic impurities.

All other liquid reagents, such as toluene and methanol, were used as received from commercial sources with purities in excess of 99 mol %. Carbon monoxide and hydrogen were obtained from Matheson as a blend gas in a standard cylinder in which the composition of each component was nearly 50 mol %. The actual composition was determined by using a Carle Series SX gas analyzer, which gave the following results: 49.14% CO , 49.6% H_2 , 1.26% (balance) N_2 , O_2 , and water.

Reaction Technique. A typical hydroformylation reaction experiment was initiated by charging a premixed solution containing the dissolved polybutadiene, toluene reaction solvent, rhodium catalyst precursor, and excess triphenylphosphine from a sealed bottle to the autoclave using an inert gas purge. The 0.3-L autoclave head was then installed and the magnetically driven head purged with additional inert gas to displace any air present in the bearing support area. The autoclave was then pressurized to about 345 kPa with the CO/H_2 blend gas and stirred for several minutes to saturate the liquid mixture with the gas. The stirring was then stopped, a leak check was performed, and the autoclave was slowly vented to atmospheric pressure. The above procedure was repeated at least twice to displace any dissolved air that was present in the liquid. Next, the stirring was set to 1000 rpm and the reactor was slowly heated up to the desired reaction temperature under low (ca. 345 kPa) CO/H_2 reactant gas pressure. Once the temperature had stabilized, the reactor pressure was quickly increased to 2066 kPa (300 psig) by using the Tescom pressure regulator. After a predetermined pressure drop occurred in the small reservoir, which corresponded to an assumed degree of polymer functionalization, the reaction was terminated by directing cooling water through the internal coils of the autoclave. A sample of the crude hydroformylated reaction product was collected, subjected to post treatment and analyzed as described below.

Reaction Product Post Treatment. Separation of the rhodium catalyst and excess triphenylphosphine from the crude hydroformylated product was performed by using methanol as a solvent through batchwise extraction. Thus, the dropwise addition of methanol to a well-stirred mixture would result in polymer precipitation, leaving the catalyst, triphenylphosphine, toluene, and excess methanol in the liquid solution phase. By recovering the polymer product and adding sufficient toluene to produce a homogeneous mixture, the above procedure could be repeated several times until a catalyst-free product was obtained. Removal of excess solvent trapped in the polymer was performed by vacuum evaporation at 1 torr and $T = 313$ K (40 °C). Elemental analysis of the final polymer product using atomic absorption showed that less than 10 ppm of rhodium was present.

Analytical Section

Both the reactant polybutadienes and the corresponding hydroformylated products were analyzed by using IR spectroscopy, NMR spectroscopy, and gel permeation chromatography. The latter two techniques were used most

often to obtain quantitative results and are described below.

NMR Spectroscopy. Both ^1H and ^{13}C NMR spectra were obtained at the Monsanto Physical Sciences Center on Varian 90-MHz continuous wave or 300-MHz Fourier transform instruments. All of the experiments were performed with 4–5 wt % of polymer in deuteriochloroform (CDCl_3) as the solvent. Optimal values of the instrument operating parameters were obtained in a series of test runs and used to obtain the NMR spectra of all reaction samples.

GPC Analysis. Molecular weight averages and compositional heterogeneity were determined by using a three-detector size-exclusion chromatography/low-angle laser light scattering (SEC/LALLS) system. The system consisted of a pump (Waters Associates, Model 590), three styrene-divinylbenzene columns connected in series with mean permeabilities of 1000, 100, and 50 Å, respectively (Polymer Laboratories), a low-angle laser light scattering (LALLS) detector (LDC/Milton-Roy, Model CMX-100), a differential refractive index (DRI) detector (Waters Associates, Model R410), and an ultraviolet absorption (UV) detector (Kratos, Model 757).

The time delay between detectors was measured with a monodisperse polystyrene standard (Polymer Laboratories) having a molecular weight of 10 000. The delay time between the LALLS and DRI detectors was found to be 27 s, while the corresponding value between the UV and DRI detectors was found to be 24 s. These values were used in subsequent calculations involving the molecular weight averages.

The SEC/LALLS system was typically equilibrated with UV grade tetrahydrofuran (THF) at a flow rate of 1 mL/min before performing any chromatographic experiments. The sample solutions were prepared by using polymer concentrations varying from 4 to 6 mg/mL in a solvent mixture containing 95% THF and 5% methanol. The latter component was added to eliminate or minimize intermolecular dimerization of the polymer-bound aldehyde functional groups. Prior to injection into the SEC/LALLS system, the sample solutions were heated to 318 K (45 °C) for 1 h. A sample injection volume of 100 μL was used.

The SEC/LALLS system was interfaced to a Digital Equipment Corporation PDP 11/23 microcomputer, which routinely collected all raw detector output data and performed all molecular weight calculations by using a standard computer program. A detailed description of the overall methodology and governing relationships used is given in Appendix A. The program output includes such items as the polymer molecular weight distribution, the various polymer molecular weight averages, and other related molecular weight distribution calculations.

Results and Discussion

Polymer Analysis by NMR. ^{13}C NMR spectroscopy of selected aldehyde monomer substrates was used to define the regiochemistry of formyl-functionalized hydroformylation products. For the specific class of products encountered in this work, butyraldehyde and 2-ethylhexanal were selected as model compounds for end-branched and internal hydroformylation. The end-branched aldehyde has a ^{13}C NMR chemical shift at 201.9 ppm, while the internal aldehyde has a ^{13}C NMR shift at 204.4 ppm. Similarly, ^1H NMR spectroscopy of the aldehyde functional groups was used to identify the regioisomers in the hydroformylated products derived from 1,2-polybutadiene, 1,4-polybutadiene, and the LX-16 (12 wt % 1,2- and ca. 88 wt % 1,4-polybutadiene) polybutadiene systems. Quantitative ^1H NMR data were also used to evaluate the fraction of polybutadiene chain units func-

tionalized with aldehyde groups.

NMR Analysis of 1,2-PBD and the Hydroformylated Product. The ^1H NMR spectrum of the 1,2-syndiotactic PBD and the hydroformylated product are compared in Figure 4. The reaction conditions used in this case are given in the figure caption. The paraffin protons occur in the 1–1.8 ppm range, while the olefinic protons are observed in the 4.7–5.6 ppm range. Protons associated with residual toluene reaction solvent in the product are seen in the 6.7–7.4 ppm range and as a singlet at 2.3 ppm. A broad peak is observed in the ^1H NMR of the product at 9.7 ppm and ^{13}C NMR shift at 202.39 ppm, which corresponds to the terminal-branched aldehyde. The small shoulder peak at ca. 9.5 ppm is the iso-branched aldehyde. This suggests that hydroformylation of 1,2-polybutadiene under these conditions occurs primarily through an anti-Markownikoff addition reaction.⁸

Confirmation that the hydroformylation is selective with negligible side reactions is provided by integration of the ^1H NMR peaks in the aldehyde and olefin region and comparison of the results to the CO/H_2 gas uptake. The results show that the percentage of terminal olefins that have been hydroformylated is 22.2% by ^1H NMR and 19.96% by gas uptake, corresponding to an absolute difference of only 2.24%. Gas uptake measurements provide a straightforward method for assessing the overall degree of polybutadiene aldehyde group functionalization in this case.

NMR Analysis of 1,4-PBD and the Hydroformylated Product. The ^1H NMR spectrum of the 1,4-*cis*-PBD and the hydroformylated product are compared in Figure 5. The protons associated with the allylic groups yield a peak at about 2.2 ppm, while the olefinic protons yield a peak at 5.4 ppm. The protons associated with the aldehyde functionality produce a peak at 2.3 ppm and another at 9.4 ppm. Peaks associated with the paraffinic protons occur in the 1.0–1.8 ppm range. Residual methanol left in the polymer during the recovery step yields a peak at 3.5 ppm and should be ignored. Collectively, these results suggest that the hydroformylation of 1,4-*cis*-polybutadiene, for the reaction conditions used here, occurs according to the stoichiometry given above by eq 1 where the aldehyde addition occurs on the internal double bond.

Integration of the ^1H NMR peaks in the aldehyde and olefin region gives that 53.96% of the olefin units are hydroformylated. This is in excellent agreement with a value of 54% obtained from the interpretation of the CO/H_2 gas uptake data.

The above results for 1,2-syndiotactic polybutadiene and 1,4-*cis*-polybutadiene demonstrate that $\text{HRhCO}(\text{PPh}_3)_3$ catalyst, when used with a sufficient excess of PPh_3 , will provide selective hydroformylation of the olefin functionality to the corresponding aldehyde product. Mohammadi and Rempel⁴ used $\text{HRhCO}(\text{PPh}_3)_3$ catalyst precursor without excess PPh_3 to hydroformylate polybutadienes containing 90% 1,2-olefin units with number-average molecular weights between 9000 and 50 000. Quantitative results on the polybutadiene conversion and selectivities to the hydroformylated products were not reported so that a direct comparison of results is not possible, however.

NMR Analysis of Mixed Polybutadiene and the Hydroformylated Product. The LX-16 polybutadiene, which is a mixture of 1,2- and 1,4-polybutadiene polymers, was first analyzed by using both ^{13}C and ^1H NMR. The ^1H NMR is shown in Figure 6a. From quantitative interpretation of both the ^{13}C and ^1H NMR spectra, it was determined that the LX-16 contained 12 wt % 1,2-

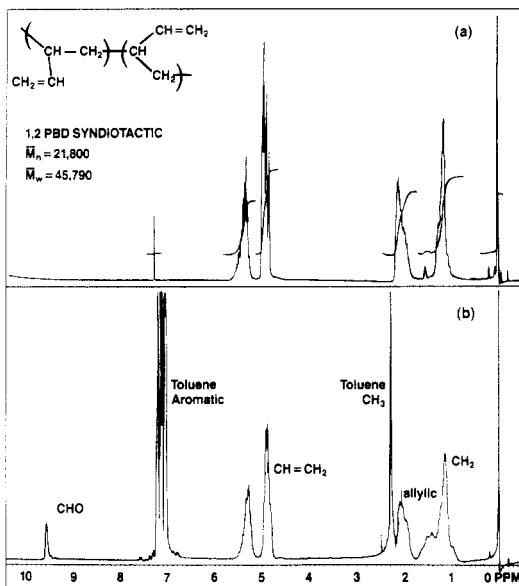


Figure 4. ^1H NMR spectra of 1,2-syndiotactic polybutadiene (a) and the hydroformylated product (b). Reaction conditions: $C_{\text{PO}} = 0.52 \text{ mol/L}$, $C_{\text{cat}} = 4 \times 10^{-4} \text{ mol/L}$, $\text{PPh}_3/\text{Rh (M)} = 165/1$, $P = 2066 \text{ kPa (gauge)}$, $\text{CO}/\text{H}_2 = 1/1$, $T = 361 \text{ K}$, solvent = toluene.

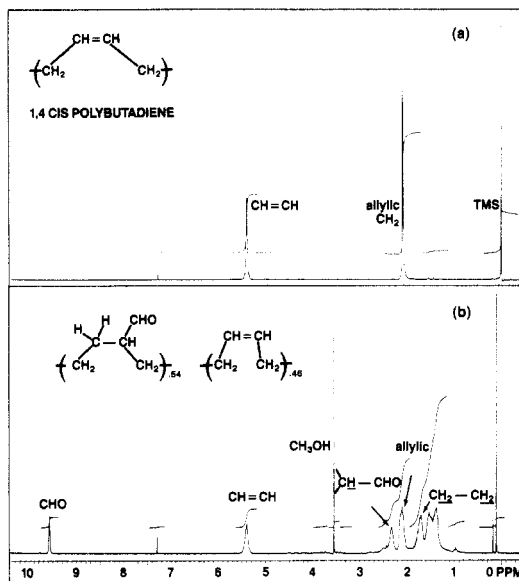


Figure 5. ^1H NMR spectra of 1,4-*cis*-polybutadiene (a) and the hydroformylated product (b). Reaction conditions: $C_{\text{PO}} = 0.55 \text{ mol/L}$, $C_{\text{cat}} = 4 \times 10^{-4} \text{ mol/L}$, $\text{PPh}_3/\text{Rh (M)} = 165/1$, $P = 2066 \text{ kPa (gauge)}$, $\text{CO}/\text{H}_2 = 1/1$, $T = 361 \text{ K}$, solvent = toluene.

polybutadiene and 88 wt % 1,4-polybutadiene. These percentages are within the ranges of 10–15 wt % 1,2-PBD, 50–60 wt % 1,4-*trans*-PBD, and 25–35 wt % 1,4-*cis*-PBD stated by the manufacturer. As expected, the ^1H NMR spectrum of LX-16 has peaks that appear at the same location as those for the 1,2- and 1,4-PBD given in Figures 4a and 5a, respectively. The magnitudes of the corresponding peaks differ as expected since the rel-

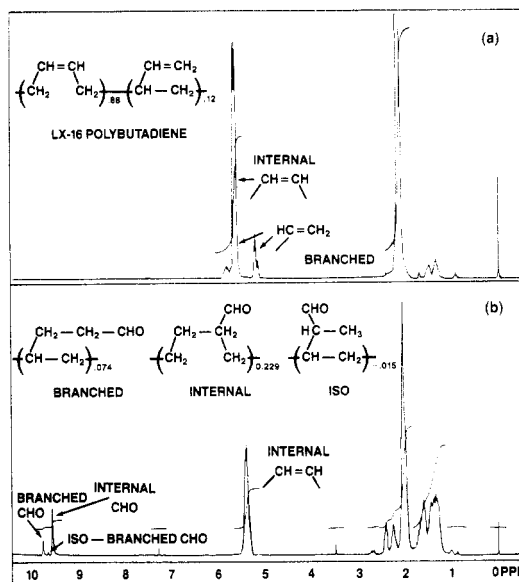


Figure 6. ^1H NMR spectra of LX-16 mixed polybutadiene (a) and the hydroformylated product (b). Reaction conditions: $C_{\text{PO}} = 8.05 \text{ mol/L}$, $C_{\text{cat}} = 4.402 \times 10^{-4} \text{ mol/L}$, $\text{PPh}_3/\text{Rh (M)} = 163/1$, $T = 353 \text{ K}$, $P = 2066 \text{ kPa (gauge)}$, $\text{CO}/\text{H}_2 = 1/1$, solvent = toluene.

ative concentrations of 1,2-PBD and 1,4-PBD in the LX-16 are not the same as those given in Figures 4 and 5.

Comparisons of the ^1H NMR spectra of the LX-16 PBD and the hydroformylated product are given in Figure 6 for the case where 32% of the olefin units have been converted. The hydroformylation reaction conditions are summarized in the figure caption. The spectrum shown in Figure 6b shows that two major aldehyde products and one trace aldehyde product are present. The broad peak at 9.5 ppm relative to CDCl_3 and corresponding ^{13}C NMR shift at 204.66 ppm are assigned to the internal aldehyde associated with the hydroformylation of the 1,4-*cis*- + 1,4-*trans*-polybutadiene chains. This value for the ^{13}C NMR shift is in excellent agreement with the value of 204.4 ppm given above for the 2-ethylhexanal model compound. The other major product appears as a broad multiplet at 9.72 ppm relative to CDCl_2 , which has a corresponding ^{13}C NMR chemical shift at 202.1 ppm. This latter value agrees well with the value of 201.9 ppm given above for butyraldehyde, which is a model compound for addition of an aldehyde to a branched terminal olefin. This peak would be associated with the hydroformylation of the 1,2-polybutadiene chains present in the LX-16 mixture. The trace peak located at 9.65 ppm has a proton that is most likely associated with the iso-branched aldehyde. This product is formed in parallel with the terminal branched aldehyde from the 1,2-polybutadiene fraction of the LX-16 through a series reaction involving isomerization of the terminal- and iso-branched aldehydes or a combination of the two pathways.

On the basis of the above results, the following reactions occur during the hydroformylation of LX-16 under the indicated conditions. According to eqs 3 and 4,

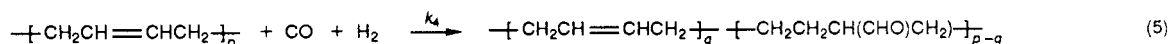
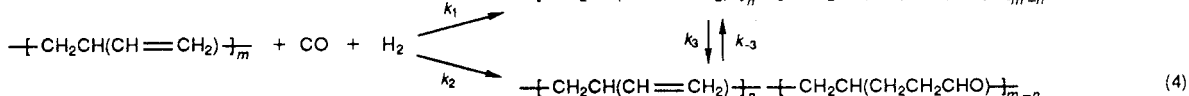
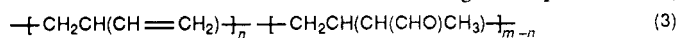


Table II
Comparison between ^1H NMR and CO/H_2 Gas Uptake Data for Evaluation of the Overall Degree of LX-16 Polybutadiene Conversion to the Corresponding Hydroformylated Product^a

% of olefin units hydroformylated by		
gas uptake	^1H NMR	abs diff, ^b %
10	10.1	0.1
20	19.1	0.9
40	39.5	0.5
80	78.3	1.7

^a Conditions: $C_{\text{PO}} = 8.05 \text{ mol/L}$, $C_{\text{cat}} = 4.402 \times 10^{-4} \text{ mol/L}$, $T = 353 \text{ K}$, $P = 2066 \text{ kPa}$, 1:1 CO/H_2 , $\text{PPh}_3/\text{Rh} (\text{M}) = 163$. ^b Defined as $100|(\text{gas uptake}) - (^1\text{H NMR})|$.

Table III
Polymer Molecular Weight Averages for LX-16 and Various Hydroformylated Products^a

polymer	\bar{M}_n	\bar{M}_w	\bar{M}_z	$p = \bar{M}_w/\bar{M}_n$
LX-16	5200	7 200	8 800	1.385
10% CHO	8000	10 101	14 400	1.263
40% CHO	9800	16 700	89 400	1.704
80% CHO	21800	103 300	762 800	4.739

^a Conditions: $C_{\text{PO}} = 8.05 \text{ mol/L}$, $C_{\text{cat}} = 4.402 \times 10^{-4} \text{ mol/L}$, $T = 353 \text{ K}$, $P = 2066 \text{ kPa}$, 1:1 CO/H_2 , $\text{PPh}_3/\text{Rh} (\text{M}) = 163$. All reported values are the average of three determinations except for LX-16, which are the average of two determinations.

hydroformylation of the 1,2-polybutadiene produces both isobranched and terminal-branched aldehyde products through series-parallel reactions. For the reaction conditions used here, formation of the latter one is highly favored. Equation 5 shows that 1,4-polybutadiene results in the formation of an internally branched aldehyde product. These observations are consistent with results reported by Pruett and Smith¹² for hydroformylation of monomer olefins.

Experimental evidence that the hydroformylation of LX-16 produces essentially 100% selectivity to aldehyde products over a large range of olefin conversion was also examined. The results of one such study are given in Table II where the overall olefin conversion obtained by gas uptake data is compared to that obtained by quantitative ^1H NMR. The absolute differences between the two methods are less than 2%, which is excellent considering that each determination represents a separate experiment. Possible side products, such as polyalcohols formed by hydrogenation of the polyaldehydes, were not detected in ^{13}C NMR spectrum. Use of the batch autoclave gas uptake data to obtain the instantaneous values for the overall polybutadiene and polyaldehyde concentrations, and hence the instantaneous value of the overall hydroformylation reaction rate, appears to be justified. Concentrations and hydroformylation reaction rates of 1,2-polybutadiene and 1,4-polybutadiene in the LX-16 mixture cannot be obtained solely from the overall gas uptake data, however, since their relative contributions cannot be isolated.

Polymer Analysis by GPC. The effect of aldehyde group addition on the molecular weight distribution of the hydroformylated products was also experimentally studied to obtain a more fundamental understanding of the resulting polymer microstructure.

Molecular weight averages for LX-16 polybutadiene and three of the hydroformylated products upon which the results in Table II are based are compared in Table III. As explained above, both quantitative ^1H NMR and gas uptake data showed that 10 wt %, 40 wt %, and 80 wt % of the olefin units had been converted to either ter-

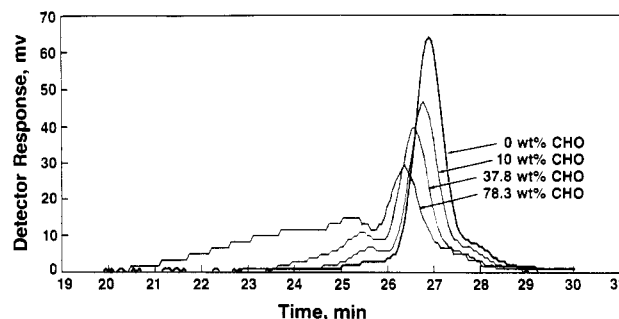


Figure 7. Gel permeation chromatograms of LX-16 mixed polybutadiene and various hydroformylation products based upon the differential refractive index (DRI) detector. Reaction conditions: $C_{\text{PO}} = 8.05 \text{ mol/L}$, $C_{\text{cat}} = 4.402 \times 10^{-4} \text{ mol/L}$, $\text{PPh}_3/\text{Rh} (\text{M}) = 163/1$, $T = 353 \text{ K}$, $P = 2066 \text{ kPa}$ (gauge), $\text{CO}/\text{H}_2 = 1/1$, solvent = toluene.

minally branched or internal aldehydes. The results in Table III show that the molecular weight averages increase with increasing degree of aldehyde addition relative to the LX-16 parent polymer. The chromatograms obtained from the differential refractive index detector are displayed in Figure 7. These show that the aldehyde functionalization of the polymer produces a bimodal molecular distribution with a shift toward the higher molecular weight components with increasing functionalization.

An increase in the polymer molecular weight averages is expected since the addition of a one aldehyde functionality will increase the molecular weight of the olefin unit from 54 g/mol to 84 g/mol. However, the observed molecular weight increases were larger than expected for the measured overall degree of hydroformylation. This is particularly apparent when comparing the polymer molecular weight averages and polydispersity for the 40% and 80% functionalized polymers. These findings suggest that the functionalized polymers either cross-link during the hydroformylation or that they associate in dilute solution to form aggregates of individual polymer molecules.

It is tempting to partially attribute the observed increases in the polymer molecular weight averages mentioned above to the increase associated with the hydrodynamic volume of the polymer that occurs with increased functionalization. While the hydrodynamic volume of the polymer does increase during the course of the hydroformylation reaction experiment due to aldehyde addition, the SEC/LALLS method automatically accounts for this since it provides an absolute measure of the polymer molecular weight. For this reason, the measured increases in the polymer molecular weight averages reported in Table III cannot be attributed, either in a partial or total sense, to increases in the polymer hydrodynamic volume. This provides further evidence that polymer cross-linking and aggregation become more pronounced with increased conversion of olefin units to aldehyde functionalities.

The nature of polymeric material giving rise to high molecular weight modes was investigated further by comparing chromatograms generated by the differential refractive index and ultraviolet absorption detectors. A wavelength of 310 nm was found to minimize the UV detector response to the olefin units while providing the maximum sensitivity to the aldehyde groups. A comparison of the chromatograms produced by the UV detector that have been normalized for mass differences is given in Figure 8. This shows that the UV detector response increases with an increase in the addition of aldehyde groups to the polymer chains.

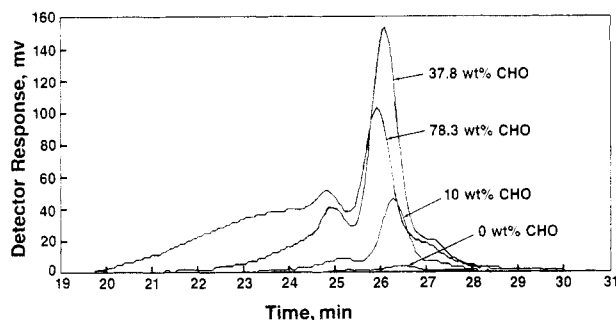


Figure 8. Gel permeation chromatograms of LX-16 mixed polybutadiene and various hydroformylation products based upon the ultraviolet (UV) detector. Reaction conditions and reaction times are the same as in Figure 7.

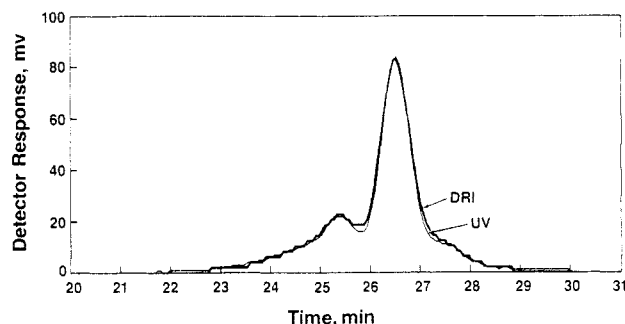


Figure 9. Comparison of gel permeation chromatograms obtained from different refractive index (DRI) and ultraviolet absorption (UV) detectors for a selected LX-16 mixed polybutadiene hydroformylation product obtained after applying mass and delay time corrections. Reaction conditions are the same as in Figure 7. The reaction time was 714 min, corresponding to the 37.8 wt % aldehyde product.

By accounting for the differences in the delay times between the DRI and UV detectors and by normalizing the DRI and UV based chromatograms for each hydroformylated product, it was possible to compare the molecular weight distribution of the aldehyde relative to that of the total polymer. Figure 9 shows the results for the polybutadiene having 40 wt % aldehyde functionalization, which is representative of those having 10–80 wt % functionalization. A comparison of the detector responses over the indicated range of elution times shows that the ratio of responses yields a value of unity with errors that are within the experimental measurements and the noise level of the detectors.

The nearly perfect overlap of the DRI and UV chromatograms suggests that the addition of aldehyde to the polybutadiene olefin units is not biased toward a particular fraction of the polybutadiene molecular weight distribution. Instead, the hydroformylation appears to occur such that the rate of aldehyde addition is constant, or nearly constant, across the entire range of molecular weight fractions that comprise the polymer. From a catalysis perspective, this suggests further that the active forms of the rhodium catalyst in solution are unbiased in terms of their hydroformylation activity for a polymer fraction of a given molecular weight. These results also suggest that the active form of the rhodium catalyst does not remain attached to a particular chain due to proximity effects, which might introduce a bias to the polymer-catalyst complex.

It is worth noting that under certain reaction conditions, the polymer product would undergo gelation in the autoclave. Precise limits on reaction conditions where gelation would occur were not defined, however. In general, use of high initial concentrations of polybutadiene

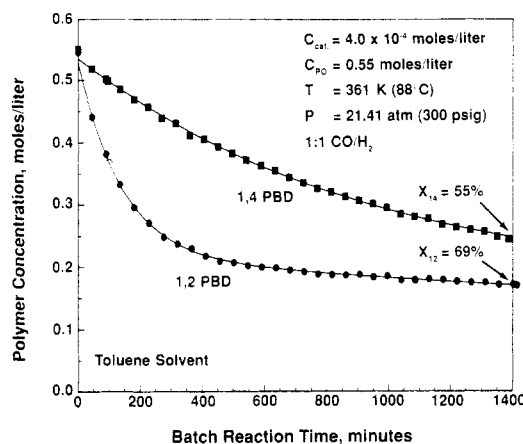


Figure 10. Comparison of total olefin concentration versus time batch reaction results for 1,4-*cis*-polybutadiene and 1,2-syndiotactic polybutadiene.

($\geq 9 \text{ mol L}^{-1}$) and high conversion ($\geq 90\%$) of the polybutadiene to the hydroformylated product provided one set of conditions that could lead to gelation. Examination of the gelation product by ^{13}C NMR showed the presence of a significant amount of acetal groups. In certain experiments where gelation did not occur, ^{13}C NMR spectra of the hydroformylated product showed minor peaks that could be assigned as acetals. These groups, in addition to the aldehydes, could be reactive sites for cross-linking. Additional characterization and experiments will be needed to resolve this issue.

Reaction Kinetics. Interpretation of CO/H_2 gas uptake rate data for a set of batch autoclave experiments was also performed. The objective here was not to perform a detailed kinetic study since this is lengthy enough to be the subject of a separate study. Instead, a relative comparison was made of the hydroformylation reaction rates for the syndiotactic 1,2-PBD, the *cis*-1,4-PBD, and the LX-16 mixed PBD under a selected set of conditions. Details of the data reduction procedure used are given in Appendix B.

Figure 10 gives a comparison of the polybutadiene olefin unit concentration versus time data for the hydroformylation of *cis*-1,4-polybutadiene and syndiotactic 1,2-polybutadiene. Estimates of the gas-liquid mass transfer resistance using the approach described by Ramachandran and Chaudhari¹³ showed that the overall rate of reaction was dominated by the intrinsic kinetics. Over a limited range of olefin conversion, the hydroformylation reaction rate for the pure 1,2-PBD and 1,4-PBD in toluene solvent can be described by apparent first-order kinetics:

$$R_{14} = -\frac{dC_{14}}{dt} = k_{14}C_{14} \quad (6)$$

and

$$R_{12} = -\frac{dC_{12}}{dt} = k_{12}C_{12} \quad (7)$$

where k_{14} and k_{12} are the pseudo-first-order reaction rate constants. For the data given in Figure 10, $k_{14} = 7.1 \times 10^{-4} \text{ min}^{-1}$ and $k_{12} = 4.137 \times 10^{-3} \text{ min}^{-1}$ so that $R_{12}/R_{14} = 5.827$ at $t = 0$. Thus, the hydroformylation of 1,2-PBD has an initial rate that is about six times faster than that for the hydroformylation of 1,4-PBD. This difference can be attributed to either the differences in the inherent activity of the rhodium catalyst to activate an internal olefin versus a terminal olefin, differences in the molecular weight of the 1,2-PBD versus 1,4-PBD, or some

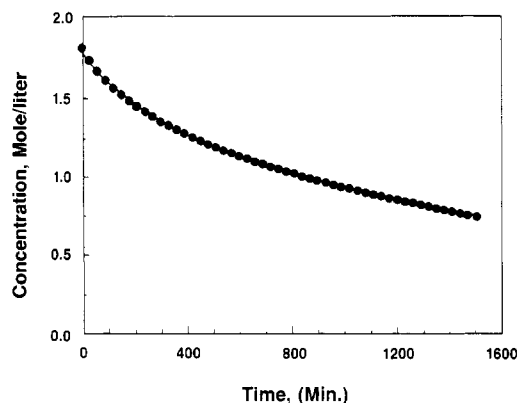


Figure 11. Comparison of experimental and model-predicted values of the total olefin concentration versus time results for the hydroformylation of LX-16 mixed polybutadiene. Parameter values: $C_{12}(t=0) = 0.3373$ mol/L, $C_{14}(t=0) = 1.4446$ mol/L, $k_{12} = 0.4221 \times 10^{-2} \text{ min}^{-1}$, $k_{14} = 0.4369 \times 10^{-3} \text{ min}^{-1}$. Reaction conditions: $C_{PO} = 1.809$ mol/L, $C_{cat} = 3.54 \times 10^{-4}$ mol/L, $PPh_3/Rh(M) = 165/1$, $P = 2066$ kPa (gauge), $CO/H_2 = 1/1$, $T = 360$ K, solvent = toluene.

combination of the two. Since 1,2-PBD's and 1,4-PBD's having the same molecular weight distribution and hence molecular weight averages are not available, a true comparison of the rates for these two PBD's where the only differences are the olefin unit structures is not feasible. By analogy to olefin monomer hydroformylation rates reported in the literature for terminal versus internal branched olefins (cf. Table 1.3.2 in Cornils⁸), one can speculate that the differences in rates are primarily due to the olefin unit structure.

Having established that the syndiotactic 1,2-polybutadiene and *cis*-1,4-polybutadiene react at noticeably different rates, this information can be used to interpret some results for the LX-16 mixed polybutadiene. Since the LX-16 contains 12 wt % 1,2-polybutadiene and 88 wt % 1,4-polybutadiene, taking ratios of the rate equations given by eqs 6 and 7 and accounting for the differences in the initial concentrations yield $R_{12}/R_{14} = 0.79$ as initial values for the relative rates in the LX-16 mixture. This suggests that the 1,2-polybutadiene component in LX-16 will account for about $100(0.79)/1.79 = 44\%$ of the overall initial rate, while the 1,4-polybutadiene will contribute the difference, or 56%, to the overall initial rate. Due to the close proximity of these initial rates, one cannot assume that the initial rate in LX-16 hydroformylation is dominated by the contribution of 1,2-polybutadiene. In view of the results presented in Figure 10, such an assumption would appear to be correct.

The integrated forms of eqs 6 and 7 show that the instantaneous concentration of the olefin unit in the LX-16 polymer will be given by the sum of the concentrations of the 1,4-olefin units and the 1,2-olefin units

$$C_{ole}(t) = C_{14,0}e^{-k_{14}t} + C_{12,0}e^{-k_{12}t} \quad (8)$$

As in the previous case, eq 8 assumes pseudo-first-order behavior and is not based upon any fundamental polybutadiene hydroformylation reaction mechanism. Numerical values for the initial concentrations $C_{12,0}$ and $C_{14,0}$ as well as the kinetic rate constants k_{12} and k_{14} were determined by exponential series parameter estimation using a modified form of subroutine BSOLVE,¹⁴ which is based upon Marquardt's method.¹⁵ A comparison of the experimental and predicted values of the olefin unit concentration is shown in Figure 11 where excellent agreement is obtained. Values for the model parameters are given in the figure captions. These parameters yield R_{12}/R_{14}

$= 2.255$ at $t = 0$ so that the initial reaction rate for the 1,2-polybutadiene component in the LX-16 exceeds that for the 1,4-polybutadiene component. This suggests that most of the 1,2-PBD will react to terminal-branched aldehyde before any significant internal aldehyde functionalization occurs. Control of the final polymer properties will be dictated primarily by the degree of 1,4-polybutadiene functionalization, since this component is present in the greatest concentration in LX-16 and represents the slowest reacting component in the mixture.

Conclusions

Hydroformylation of polybutadienes can be performed by using $HRhCO(PPh_3)_3$ homogeneous catalyst precursor with excess phosphine ligand under mild reaction conditions to yield polyaldehyde products at nearly 100% selectivity. Hydroformylation of 1,4-*cis*-polybutadiene yields the internally branched aldehyde product with an initial reaction rate that is about one-sixth that for the 1,2-syndiotactic polybutadiene when compared under identical reaction conditions. This difference in rates can be attributed to the accessibility of the carbon-carbon double bond and is analogous to that observed for the hydroformylation of olefin monomers.

For the polybutadienes and reaction conditions considered in this study, the rhodium-phosphine catalyst adds the aldehyde functionality over the entire range of molecular weight at an equal probability. This suggests that the molecular configuration of the polymer in the reaction medium does not hinder the coordination of the catalyst to a reactive site on the polymer. Cross-linking of the hydroformylated product can alter the polymer molecular weight distribution, but this reaction can be reversed by exposure of the polymer to a nucleophilic solvent.

The kinetic behavior of the LX-16 model polybutadiene follows a trajectory that is a composite of those associated with the hydroformylation of the 1,2- and 1,4-polybutadiene components. It can be described by a rate equation that assumes pseudo-first-order behavior with respect to both of these components.

Appendix A. Description of the Molecular Weight Calculations

The molecular weights were calculated from light scattering intensities according to

$$\frac{Kc_i}{Ra_i} = \frac{1}{M_{w_i}} + 2A_2c_i \quad (A1)$$

Here, K is an optical constant, Ra_i is the polymer Rayleigh ratio for data point i , M_{w_i} is the weight-average molecular weight for data point i , A_2 is the second virial coefficient, and c_i is the concentration for data point i . The second virial coefficient A_2 is assumed to be a constant value of 1.0×10^{-4} , while the parameters K , Ra_i , and c_i were calculated by using the expressions given below.

Values for the Rayleigh ratio Ra_i were determined from

$$Ra_i = \frac{G_{i,\theta}}{G_0} \Phi Q \quad (A2)$$

where $G_{i,\theta}$ is the LALLS detector response at a scattering angle θ for data point i , G_0 is the LALLS detector response of a scattering angle of zero, Φ is the instrumental attenuator constant, and Q is the LALLS cell constant. G_0 , Φ , and Q were 300 mV, 1.792 $\times 10^{-7}$, and 1.393, respectively, for the LALLS detector used here.

The values of c_i used in eq A1 were determined from the following expression

$$c_i = h_i M / Q_m \Delta t_i \quad (\text{A3})$$

where h_i is the normalized peak height of the DRI output response at data point i , M is the weight of the injected sample, Q_m is the volumetric flow rate of the mobile phase, and Δt_i is the time interval used to sample the detector output response.

The optical constant K that appears in eq A1 was given by

$$K = \frac{2\pi^2 \tilde{n}^2 (1 + \cos^2 \theta) (dn/dc)^2}{\lambda^4 N} \quad (\text{A4})$$

where λ is the wavelength of the incident light, \tilde{n} is the refractive index of the mobile phase at the wavelength of the incident light, N is Avogadro's number, dn/dc is the specific refractive index increment for the polymer, and θ is the light scattering angle. Values for θ and n were 5.5° and 1.405, respectively.

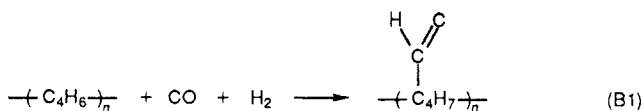
The dn/dc values used in eq A4 were determined by two methods. For the LX-16 polybutadiene, dn/dc was measured with a laser differential refractometer (Model KMX-16, LDC/Milton Roy). A dn/dc value of 0.145 mL/g was determined for LX-16 in THF at 25°C . For the hydroformylated polymers, dn/dc was determined by using the same device or by comparing mass to area (M/A) response factors from the DRI detector against the M/A response factor for LX-16. The factors were related to one another by the following expression

$$(dn/dc)_{\text{hp}} = \frac{(M/A)_{\text{LX-16}} (dn/dc)_{\text{LX-16}}}{(M/A)_{\text{hp}}} \quad (\text{A5})$$

where the subscript hp refers to the hydroformylated product. Equations A1–A5 are the key relationships used to evaluate the polymer molecular weight distribution.

Appendix B. Interpretation of the Gas Uptake Data

Examination of the polybutadiene hydroformylation reactions given by eqs 3–5 suggests that these can be written in the following general form where no distinction is made between either the internal or branched olefin unit



It follows that the global reaction rates of the olefin unit and the $\text{CO} + \text{H}_2$ blend gas are related according to

$$R_{\text{ole}} = \frac{\nu_{\text{ole}}}{\nu_{\text{CO}} + \nu_{\text{H}_2}} R_{\text{CO} + \text{H}_2} \quad (\text{B2})$$

Here, the ν_i denote the stoichiometric coefficients for CO , H_2 , and the olefin unit, respectively. Inspection of eq B1 shows that $\nu_{\text{CO}} = \nu_{\text{H}_2} = \nu_{\text{ole}} = -1$, where the negative sign is the standard convention used for reactants. Inserting the differential expressions for the global reaction rates into eq B2 and integrating show that the instantaneous total molar concentration of olefin in the reaction liquid $C_{\text{ole}}(t)$ will be given by

$$C_{\text{ole}}(t) = C_{\text{ole},0} - \frac{N_{\text{CO}+\text{H}_2}(t=0) - N_{\text{CO}+\text{H}_2}(t)}{2V_l} \quad (\text{B3})$$

In eq B3, the initial and instantaneous moles of blend

gas in the small reservoir and associated tubing are denoted by $N_{\text{CO}+\text{H}_2}(t=0)$ and $N_{\text{CO}+\text{H}_2}(t)$, respectively, while the total volume of reaction liquid is V_l . The initial total molar concentration of olefin in the reactor is denoted by $C_{\text{ole},0}$ and is given by $C_{\text{ole},0} = w_{\text{PO}}/(V_l M)$ where w_{PO} is the initial charge of polybutadiene and M is the molecular weight of the olefin unit. A value of $M = 54 \text{ g mol}^{-1}$ was used in this work.

The moles of blend gas in the small reservoir were calculated from the raw experimental values of gas temperature and total pressure shown in Figure 3. At each reaction time $t_i = i\Delta t$, the specific volume V_m of the gas was calculated by using the Marton and Hou equation of state:¹⁶

$$P = \sum_{i=1}^5 f_i (V_m - b)^{-i} \quad (\text{B4})$$

Equation B4 was solved for V_m by the Newton–Raphson method using the ideal gas specific volume $V_m^{\text{id}} = RT/P$ as the initial guess. Expressions for b and the f_i , which require the mixture critical temperature, mixture critical pressure, absolute temperature, and absolute pressure as the input parameters, are summarized in Sherwood and Reid.¹⁶ Evaluation of the mixture critical properties was performed by using the gas-phase mixing rules summarized elsewhere.¹⁷ Once the specific gas volume of the blend gas was determined, the total moles were calculated from the relation $N_{\text{CO}+\text{H}_2} = V_{\text{sr}}/V_m$ where V_{sr} is the volume of the small reservoir and the associated external tubing sensed by the pressure transducer PT #2 shown in Figure 2.

To obtain experimental values of the reaction rate in eq B2, the array of $C_{\text{ole}}(t)$ versus t values calculated from eq B3 were fitted to a two-term exponential decay function

$$C_{\text{ole}}(t) = a_1 e^{b_1 t} + a_2 e^{b_2 t} \quad (\text{B5})$$

The empirical constants a_1 , a_2 , b_1 , and b_2 were obtained by using a modified form of subroutine BSOLVE as described by Kuester and Mize¹⁴ that is based on Marquardt's method.¹⁵ Differentiation of eq B5 shows that the olefin unit reaction rate at time $t = t_i$ is given by

$$R_{\text{ole}}(t_i) = a_1 b_1 e^{b_1 t_i} + a_2 b_2 e^{b_2 t_i} \quad (\text{B6})$$

The initial rate is obtained by letting $t_i = 0$ in the above equation to yield

$$R_{\text{ole}}(t_i = 0) = a_1 b_1 + a_2 b_2 \quad (\text{B7})$$

Acknowledgment. We thank R. L. Fenton, R. A. Holub, W. A. Stultz, and J. A. Giezelmann for their assistance on various experimental aspects of this work.

Nomenclature

C_{12}	total molar concentration of the 1,2-butadiene olefin in the polybutadiene polymer, mol/L
C_{14}	total molar concentration of the 1,4-butadiene olefin in the polybutadiene polymer, mol/L
C_{ole}	total molar concentration of butadiene olefin in the polybutadiene polymer, mol/L
k_1	pseudo-first-order rate constant for 1,2-polybutadiene hydroformylation to the isobranched aldehyde product appearing in eq 3, s^{-1}
k_2	pseudo-first-order rate constant for 1,2-polybutadiene hydroformylation to the terminal-branched aldehyde product appearing in eq 4, s^{-1}

k_3, k_{-3}	pseudo-first-order rate constants for isomerization of the 1,2-polybutadiene hydroformylated product appearing in eqs 3 and 4, s^{-1}
k_4	pseudo-first-order rate constant for 1,4-polybutadiene hydroformylation to the internally branched aldehyde product appearing in eq 5, s^{-1}
k_{12}	pseudo-first-order rate constant for hydroformylation of pure 1,2-polybutadiene appearing in eq 7, s^{-1}
k_{14}	pseudo-first-order rate constant for hydroformylation of pure 1,4-polybutadiene appearing in eq 6, s^{-1}
R_{12}	reaction rate for hydroformylation of 1,2-polybutadiene defined by eq 7, mol/(L min)
R_{14}	reaction rate for hydroformylation of 1,4-polybutadiene defined by eq 6, mol/(L min)
t	reaction time, s

Subscripts

12	denotes 1,2-butadiene or 1,2-polybutadiene
14	denotes 1,4-butadiene or 1,4-polybutadiene
ole	denotes the butadiene unit

References and Notes

- (1) Cull, N. L.; Mertzweiler, J. K.; Tenney, H. M. (Esso Research and Engineering Company) U.S. Patent 3 383 426, 1968.
- (2) Ramp, F. L.; Dewitt, E. J.; Trapasso, L. E. *J. Polym. Sci.* **1966**, *4*, 2267.
- (3) Sanui, K.; MacKnight, J. W.; Lenz, R. W. *Macromolecules* **1974**, *7*, 952.
- (4) Mohammadi, N. A.; Rempel, G. L. In *Chemical Reactions on Polymers*; Benham, J. L., Kinstle, J. F., Eds.; ACS Symposium Series 364; American Chemical Society: Washington, DC, 1988; pp 373-408.
- (5) Hedrick, R. M.; Gabbert, J. D. *Reaction Injection Molding of Nylon 6 Block Copolymer*, Second World Congress of Chemical Engineering; Montreal, Canada, Oct 1981.
- (6) Hedrick, R. M.; Gabbert, J. D. Nylon Block Copolymer for a New Reaction Injection Molding System. Paper presented at the SITEV 1982 Meeting, Geneva, Switzerland, May 1982.
- (7) Gabbert, J. D.; Garner, A. Y.; Hedrick, R. M. Developments in Nylon 6 Block Copolymer RIM. Society of Automotive Engineers International Congress and Exposition, Detroit, MI, Feb 1982; SAE Technical Paper Series No. 820420.
- (8) Cornils, B. In *New Synthesis with Carbon Monoxide*; Falbe, J., Ed.; Springer-Verlag: New York, 1980.
- (9) Brown, C. K.; Wilkinson, G. *J. Chem. Soc. (A)* **1970**, 2753.
- (10) Pruett, R. L. in *Advances in Organometallic Chemistry*; Stone, F. G. A., West, R., Eds.; Academic Press: New York, 1979; Vol. 17, pp 1-60.
- (11) Balhiser, R. E.; Samuels, M. R.; Eliassen, J. D. *Chemical Engineering Thermodynamics. The Study of Energy, Entropy, and Equilibrium*; Prentice-Hall: New Jersey, 1972.
- (12) Pruett, R. L.; Smith, J. A. *J. Organomet. Chem.* **1969**, *34*, 327.
- (13) Ramachandran, P. A.; Chaudhari, R. V. *Three-Phase Catalytic Reactors*; Gordon and Breach: London, 1985.
- (14) Kuester, J. L.; Mize, J. H. *Optimization Techniques with Fortran*; McGraw-Hill: New York, 1973.
- (15) Marquardt, D. W. *Technometrics* **1970**, *12*, 591.
- (16) Sherwood, T. K.; Reid, R. F. *The Properties of Gases and Liquids*, 2nd ed.; McGraw-Hill: New York, 1968.
- (17) Mills, P. L.; Ramachandran, P. A.; Duduković, M. P. In *Reaction Engineering for Multiphase Catalyzed Systems*; AIChE Continuing Education Lecture Notes, New York, 1988; Chapter 4.

Intermediate-Angle Neutron and X-ray Scattering Functions of Poly(methyl methacrylate) Chains

Michele Vacatello,¹ Do Y. Yoon,* and Paul J. Flory²

IBM Research Division, Almaden Research Center, 650 Harry Road,
San Jose, California 95120-6099. Received August 8, 1989;
Revised Manuscript Received October 13, 1989

ABSTRACT: The molecular scattering functions of isotactic, syndiotactic, and atactic poly(methyl methacrylate) (PMMA) chains have been calculated according to the three different rotational isomeric state (RIS) models in the literature and compared with experiments. Comparison with the neutron scattering experiments on glassy (atactic) PMMA shows that only the most rigorous six-state model predicts all the features exhibited by the experimental results over the entire scattering vector q ($= (4\pi/\lambda) \sin(\theta/2)$) to ca. 0.6 \AA^{-1} . In particular, the two-state and the three-state models predict the occurrence of a second maximum in the absolute-scale Kratky plot at values of q that are considerably smaller than the experimental results. In contrast, the scattering function calculated in the framework of the six-state model shows the two maxima and the intervening minimum in the same locations of q as those in the experimental curve. The six-state RIS model also predicts the molecular scattering functions in good agreement with the available neutron scattering results on the isotactic and syndiotactic PMMA in the bulk, up to $q \approx 0.25 \text{ \AA}^{-1}$, as well as the X-ray scattering experiments on syndiotactic PMMA in solution up to $q \approx 0.7 \text{ \AA}^{-1}$. Therefore, our results show that even in the case of a complicated looking polymer like PMMA the chain conformations in the bulk amorphous state correspond very closely to the unperturbed random coils, not only for the overall chain configuration but also for local chain segments constituted by a few units.

Introduction

It is now well-known that the elastic scattering of thermal neutrons in the small and intermediate angle region

is an invaluable, unique tool to probe the overall and the local conformations of polymer molecules in a variety of environments.³ This is due to the fact that the marked difference between the coherent scattering lengths of hy-